applied sciences

MDPI

*Article*

# Starch-Polyvinyl Alcohol-Based Films Reinforced with Chitosan Nanoparticles: Physical, Mechanical, Structural, Thermal and Antimicrobial Properties

**Yahya Garavand [1], Amin Taheri-Garavand [1,*], Farhad Garavand [2,*], Feizollah Shahbazi [1], Diako Khodaei [3] and Ilaria Cacciotti [4,*]**

[1] Mechanical Engineering of Biosystem Department, Lorestan University, Khorramabad 68151-44316, Iran; yahya.garavand@gmail.com (Y.G.); shahbazi.f@lu.ac.ir (F.S.)
[2] Department of Food Chemistry and Technology, Teagasc Moorepark Food Research Centre, Fermoy, P61 C996 Co. Cork, Ireland
[3] Department of Sport, Exercise, and Nutrition, Galway-Mayo Institute of Technology (GMIT), H91 T8NW Galway, Ireland; diako.khodaei@gmit.ie
[4] Department of Engineering,, University of Rome 'Niccolò Cusano', INSTM RU, 00166 Rome, Italy
* Correspondence: taheri.am@lu.ac.ir (A.T.-G.); farhad.garavand@teagasc.ie (F.G.); ilaria.cacciotti@unicusano.it (I.C.)

**Abstract:** The main purpose of the current study was to propose innovative composite films based on a corn starch/polyvinyl alcohol (PVA) blend (starch:PVA 40:60) and loaded with 3 different levels of chitosan nanoparticles (CNPs) (1, 3, and 5% *w*/*v*) to strengthen its physical, mechanical, structural, thermal and antimicrobial attributes. The synthesized CNPs were spherical with a particle size of ca. 100 nm as demonstrated by scanning electron microscopy (SEM) micrographs and dynamic light scattering tests. The results showed that the CNPs incorporation within the starch-PVA 40:60 films promoted a uniform surface without any considerable pores. These films were characterized by a homogeneous CNP distribution within the polymer matrix, causing a significant decrease in water vapor permeability (WVP) (e.g., from 0.41 for the control film to 0.28 g·mm/kPa·h·m$^2$ for the composite film loaded with 5% CNPs). The film solubility, transparency, glass transition and melting temperatures, and elongation at break were also reduced by increasing the CNP content from 1% to 5%, while total color and tensile strength parameters increased. The antibacterial effects of CNPs were more effective against Gram-positive bacteria (*Staphylococcus aureus*) than Gram-negative bacteria (*Escherichia coli* and *Salmonella typhimurium*). It can be concluded that the addition of CNPs to the starch-PVA matrix could improve its functional and technological attributes for food packaging applications.

**Keywords:** polyvinyl alcohol; starch; chitosan nanoparticles; antibacterial effects; packaging film



**Citation:** Garavand, Y.; Taheri-Garavand, A.; Garavand, F.; Shahbazi, F.; Khodaei, D.; Cacciotti, I. Starch-Polyvinyl Alcohol-Based Films Reinforced with Chitosan Nanoparticles: Physical, Mechanical, Structural, Thermal and Antimicrobial Properties. *Appl. Sci.* **2022**, *12*, 1111. https://doi.org/10.3390/app12031111

Academic Editor: Luis Rojo del Olmo

Received: 18 December 2021
Accepted: 18 January 2022
Published: 21 January 2022



## 1. Introduction

Petroleum-based polymers are the primary materials used in the packaging industry. The environmental, ecological, and safety concerns over petroleum-based polymers have raised a global trend in the use of biodegradable polymers [1]. Biodegradable plastics can be obtained from either synthetic or natural polymers. Synthetic polymers are commonly derived from non-renewable petroleum resources, while natural polymers are derived from natural/renewable sources or the by-products of food and agricultural products [2]. Biodegradable plastics can be degraded into carbon dioxide ($CO_2$), methane ($CH_4$), water, and inorganic compounds by the natural microorganisms present in soil or water [3] and can be used to produce edible films and coatings that have a wide application in the food industry due to their biodegradability, sustainability, mechanical, and barrier properties [4]. Moreover, these biopolymers can be used as carriers for flavours, nutrients, vitamins, antioxidants, and antimicrobial agents [5]. Synthetic polymers are more applicable in the

packaging industry compared to natural polymers mainly due to their mechanical and barrier properties. However, several efforts are currently dedicated to the development of packaging materials based on natural biopolymers, such as polysaccharides, proteins, etc. [6–8]. Among them, starch is a novel biopolymer to replace conventional plastics in food packaging due to its high biodegradability, abundance in nature, chemical stability, and film-forming ability. It is one of the most abundant and cheap natural biopolymers made from glucose units that are formed in amylose and amylopectin structures. Starch's functional properties are mainly due to the amylose and amylopectin forms with high molecular weights and their physical form in the granular structure of starch [9]. Starch is a thermoplastic material and can form films in the presence of food-grade plasticizers such as polyols (glycerol, sorbitol, xylitol, etc.), sugars (glucose, fructose, etc.), and water [10]. During the starch heating gelation, the hydrogen bonds supporting the crystal structure of the granules break down, and the plasticizers prevent the recrystallization and improve the integrity of starch films by positioning between starch chains' hydrogen bonds. However, starch films have weaker mechanical and barrier properties compared to conventional polymers such as polyethylene [11]. Thus, additives or modification strategies have been proposed to improve the mechanical and barrier properties of starch films [11], such as blending with synthetic polymers and reinforcing with suitable nanofillers [7,12,13].

Among synthetic polymers, hydrophilic ones, such as poly(vinyl alcohol) (PVA), are generally safer to use and cheaper than hydrophobic polymers due to using polar solvents such as water and ethanol during the moulding technique. Poly(vinyl alcohol), which is commercially produced from the hydrolysis of poly(vinyl acetate) under alkaline conditions [14], is widely used in the food industry as a packaging material, film, and more often, lacquer due to its low permeability to gases [15].

Nano-scale reinforcing materials are a class of filler materials used to modify polymer matrices by improving their mechanical, thermal, and barrier properties [16]. Chitosan is the second most common biopolymer available in nature, and it is the main component of the exoskeletons of arthropods [2]. Chitosan, due to possessing a considerable antioxidant, antimicrobial activity, and biodegradability, has wide applications in the food industry, agriculture, medicine, and the cosmetics industry [17]. Moreover, chitosan nanoparticles (CNPs), by virtue of their high surface area, biocompatibility, low toxicity, and film-forming ability, have gained attention as potential nanofillers in different polymers [18]. Many studies have reported that the addition of CNPs improved the tensile strength, storage modulus, thermal properties, and barrier properties of films while the elongation at break reduced [19–21].

In this framework, the aim of this research was to characterize a novel biodegradable nanocomposite material based on a starch-PVA blend loaded with CNPs for food packaging applications. The effect of incorporating CNPs into starch-PVA films in terms of physical, mechanical, thermal, and structural properties was fully investigated. The antimicrobial properties of the films against Gram-positive bacteria (*Staphylococcus aureus*) and Gram-negative bacteria (*Escherichia coli* and *Salmonella typhimurium*) were also evaluated.

## 2. Materials and Methods

### 2.1. Materials

Ethanol (95%), medium molecular weight chitosan (~450 kDa and deacetylation degree of 85%), and sodium tripolyphosphate (STPP) were obtained from Merck Co. (Darmstadt, Germany). Starch (from corn, with 0.5% ash and 25% amylose) was provided from Glucosan Co. (Tehran, Iran). Stock cultures of *Echerichia coli* PTCC 1330 (*E. coli*), *Staphylococcus aureus* PTCC 1764 (*S. aureus*), and *Salmonella typhimurium* PTCC 1609 (*S. typhimurium*) were obtained from the Persian Type Culture Collection (PTCC) (Tehran, Iran). Other chemicals were of analytical grade.

### 2.2. Chitosan Nanoparticles (CNPs) Preparation

Chitosan nanoparticles were prepared through the anisotropic gelation between chitosan and STPP. For this aim, chitosan powder was dissolved in 1% (*v*/*v*) acetic acid, and after 24 h of mixing, it was filtered using filter paper to remove the impurities. Afterward, STPP solution (1% *w*/*v*) was gradually added to the chitosan solution and stirred at 1000 rpm for 40 min. The resulted suspension was centrifuged (CF16RXII Hitachi Centrifuge, Tokyo, Japan) at 12,000× *g* for 20 min, and the sediment was washed with distilled water, freeze-dried and kept at the fridge prior to experiments [20,21].

### 2.3. Nanocomposite Films Preparation

Films were prepared using the solvent casting method as described by Khazaei et al. [22]. Briefly, starch and PVA were mixed in a 40:60 ratio (selected as per pre-tests on different ratios of starch and PVA). Afterward, the mixture was dissolved in distilled water (2% *w*/*v* and 3% *w*/*v* for starch and PVA, respectively) and stirred at 400 rpm for 1 h during heating at 95 °C. Film-forming solutions were degassed using a vacuum chamber, and the impurities were displaced using Whatman No. 3 filter paper. Afterward, glycerol (10% *w*/*w*) was added to the solution and stirred for 15 min at room temperature. CNPs were dispersed in distilled water using an ultrasonicator mixer (MSH-20A, DAIHAN Scientific, Seoul, Korea) at 80% power and 20 kHz for 30 min at room temperature and added to the film-forming solutions at different concentrations of 0, 1, 3, and 5% *w*/*v*. The film-forming solutions/suspensions were poured into Teflon petri dishes with a diameter of 15 cm. Film drying was carried out at 40 °C for 4 h in an oven. Dried films were peeled off and stored in a desiccator containing saturated calcium nitrate solution at room temperature and a relative humidity of 55% prior to experiments.

### 2.4. Characterization of CNPs

#### 2.4.1. Microstructural Analysis of CNPs

CNP morphology was evaluated using scanning electron microscopy (SEM) (H4160, Hitachi, Tokyo, Japan). To do this, freeze-dried CNPs were sputter-coated with a gold layer under an argon atmosphere (25 mA, 100 s) [23].

#### 2.4.2. Particles Size Analysis

CNP size was investigated by means of a dynamic light scattering (DLS) instrument (Zetasizer NanoZS Instrument, Malvern Instruments, Malvern, UK). CNPs were dispersed in 1% (*v*/*v*) of acetic acid solution, and the average particles size and polydispersity index were evaluated using argon laser (λ = 633 nm) with a scattering angle of 90° at room temperature [22].

### 2.5. Characterization of Nanocomposite Films

#### 2.5.1. Thickness of Films

The thickness of the films was measured using a digital micrometre (MitutoyoM820-25, Mitutoyo, Kanagawa, Japan) with an accuracy of 0.001 mm [23]. Ten points were measured at various locations of each film sample, and the results were provided as an average value ± standard deviation.

#### 2.5.2. Moisture Content and Water Solubility

The moisture content (MC) of the films was calculated based on the weight loss of samples (2.5 × 2.5 $cm^2$) upon drying in an oven at 100 °C for 24 h [23]. The results were expressed as the weight of water per 100 g of dry films (d.b.).

$$\mathrm{MC}\ (\%) = \frac{(\mathrm{M1} - \mathrm{M2})}{\mathrm{M1}} \times 100 \quad (1)$$

where M1 and M2 are the weights of the films before and after the oven drying, respectively. Three replicates were done for each film.

Moreover, solubility tests were performed by dipping the dried square films (100 °C for 24 h) in distilled water for 24 h. Afterward, films were removed from the water, and their weight was measured. The water solubility (WS) of films is calculated as a percentage using the following equation [5]:

$$\text{WS}\ (\%) = \frac{(\text{M2} - \text{M3})}{(\text{M2})} \times 100 \quad (2)$$

where M2 and M3 are the weights of the dried films before and after the solubility test, respectively. Three replicates were done for each film.

#### 2.5.3. Water Vapor Permeability

Film water vapor permeability (WVP) was calculated based on ASTM E96-65 method. Glass permeation cups with an internal diameter of 2 cm and length of 4.5 cm were used. A total of 3 g of silica gels were placed inside the cups, and then the film pieces were placed on the top of the cups and sealed using parafilm. Films were conditioned at RH of 55% for 24 h before the experiments. Glass cups sealed with the films were placed into a desiccator containing saturated potassium sulfate and stored at room temperature. The weight of glasses was recorded during time intervals. The water vapor transmission rate (WVTR) of the films was defined based on the slope of (g/s) divided by the surface area ($m^2$). WVP ($g \cdot mm/kPa \cdot h \cdot m^2$) was calculated using the equation below:

$$\text{WVP} = \frac{\text{WVTR}}{\text{P}(\text{R}_1 - \text{R}_2)} \times \text{X} \quad (3)$$

where WVTR represents the water vapor transmission rate ($g/m^2 \cdot day$), X represents the film thickness (m), P represents the saturation water pressure at 25 °C (Pa), $R_1$ represents the relative humidity in the desiccator (%), and $R_2$ represents the relative humidity in glass cups (%) [24].

#### 2.5.4. Opacity of the Films

The opacity of the films was determined using a modified standard method described by Khodaei et al. [25]. The film samples were cut into 1 × 3 $cm^2$ rectangular stripes and placed into a cuvette. The light absorbance of the films at the wavelength of 600 nm was recorded using a spectrophotometer (Kontron Uvikon 820 spectrophotometer, Kontron, Munich, Augsburg, Germany), and the films opacity was expressed by dividing the absorbance on their thickness.

#### 2.5.5. Surface Color Analysis

The color parameters, i.e., lightness (L*), red-green (a*) and yellow-blue (b*) in the CIELAB color scale, were measured by means of a Hunter lab colorimeter (Minolta CR 300 Series, Osaka, Japan). The total color difference of films (ΔE) was also calculated using the following equation [25]:

$$\Delta\text{E} = \sqrt{(\text{L}' - \text{L})^2 + (\text{a}' - \text{a})^2 + (\text{b}' - \text{b})^2} \quad (4)$$

#### 2.5.6. SEM Analysis of the Nanocomposites

The films' surface morphology was studied by using a scanning electron microscopy (SEM, Hitachi, Japan) at the accelerating voltage of 10 kV after sputter-coating with a gold layer by using an ion-sputter coater at room temperature.

#### 2.5.7. *X*-ray Diffraction (XRD)

*X*-ray diffraction patterns of the nanocomposite films were acquired using a diffractometer (X'Pert PRO, PAnalytical, Almelo, The Netherland) with a CuKα radiation source.

The scans were plotted in a 2θ diffraction angle in oscillating mode ranging from 5° to 60° at a scan speed of 2°/min with a wavelength of 0.154 nm.

#### 2.5.8. Mechanical Tests

Mechanical analysis was carried out following the D-882 standard as described by Khazaei et al. [22]. Films were cut into 15 × 100 $mm^2$ stripes and conditioned in a humidity chamber with RH of 65% and temperature of 21 °C for 24 h. A texture analyser apparatus (MTS, TA.XTPlus, Surrey, UK), fitted with 100 N load cell, was employed to measure the tensile strength (TS) and elongation at break (EAB) of the films, setting a distance between grips of 10 cm and a crosshead speed of 10 mm/min.

#### 2.5.9. Differential Scanning Calorimetry (DSC)

The thermal behaviour of the nanocomposite films was examined using a differential scanning calorimeter (DSC Q2000, TA Instrument, New Castle, DE, USA) with a sample weight of ~12 mg, temperature range from −50 °C to +200 °C, heating-cooling rate of 10 °C/min, and nitrogen flux of 40 cc/min. The melting ($T_m$) and glass transition ($T_g$) temperatures were obtained from the heating scans [13].

#### 2.5.10. Antimicrobial Properties

The agar diffusion method was used to study the antimicrobial properties of nanocomposite films against *E. coli*, *S. aureus*, and *S. typhimurium* according to the methods of Dehnad et al. [24] and Babaee et al. [26], with small modifications. For this aim, 0.1 mL of bacterial suspension containing $10^8$ CFU/mL was spread on BHI agar (Merck, Darmstadt, Germany) plates. Afterward, film discs were placed on the media and then incubated at 37 °C for 24 h. Finally, the inhibition zone area surrounding film discs was calculated by measuring its diameter.

### *2.6. Statistical Analysis*

All the experiments were conducted in triplicate, and the results were presented as mean ± standard deviation. The SPSS (V.18.1) software was employed to analyse the obtained data, and statistical analysis was carried out by one-way analysis of variance (ANOVA) using Duncan's multiple range test at the probability level of 5% ($p < 0.05$).

## 3. Results and Discussion

### *3.1. CNPs Characterization*

The morphology and diameter size distribution of the CNPs are presented in Figure 1. The SEM micrograph reveals a spherical shape for freeze-dried CNPs with a uniform size (Figure 1a). The size of CNPs ranged between 50 and 100 nm, in good correlation with results reported by Antoniou et al. [27] and smaller with respect to those reported by De Moura et al. [28], very probably due to the different synthesis conditions (lower chitosan molecular weight and a lower chitosan or TPP amount in the present study).

Figure 1b shows the particle size distribution and average size of the CNPs determined by means of DLS analysis. From the results, the polydispersity index of the synthesized CNPs was 0.191, with a mean particle size of 108 ± 5 nm. However, the dried CNPs size was smaller due to the CNPs swelling in aqueous conditions and the aggregation of some particles in this form in solution [29]. The zeta potential is another important parameter to study the stability of colloidal materials, and it was evaluated through Zetasizer NanoZS Instrument. The zeta potential of CNPs in this study was +36 mV, suggesting their colloidal stability.

### *3.2. Microstructure Analysis*

The mechanical and barrier properties of the films are influenced by the structure, morphology and integrity of the matrix [30]. These aspects were investigated by observation at SEM. The SEM micrographs of control and nanocomposite films are compared in Figure 2.

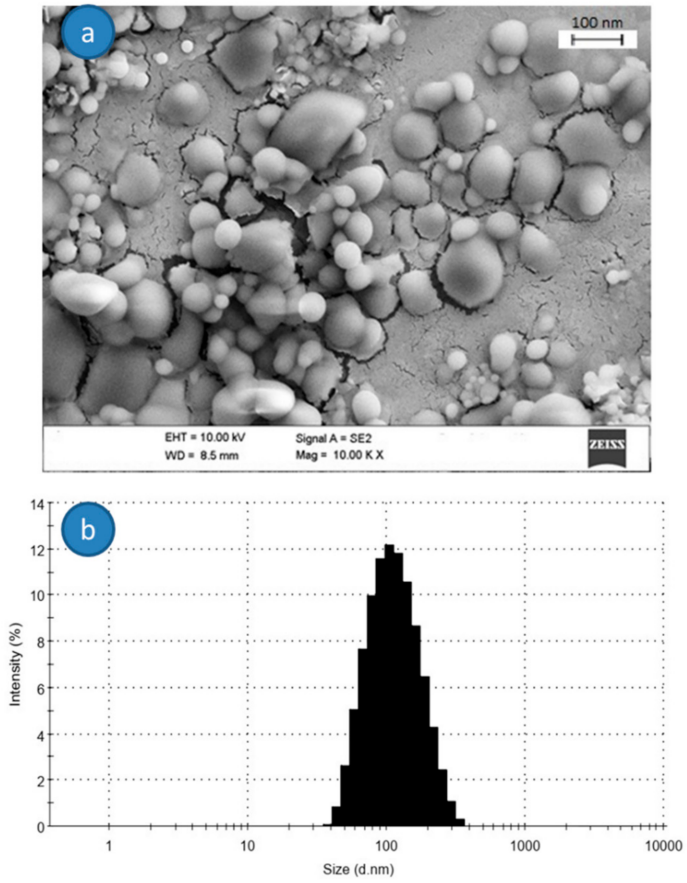


**Figure 1.** SEM micrograph (**a**) and particle size distribution (**b**) of freeze-dried CNPs.

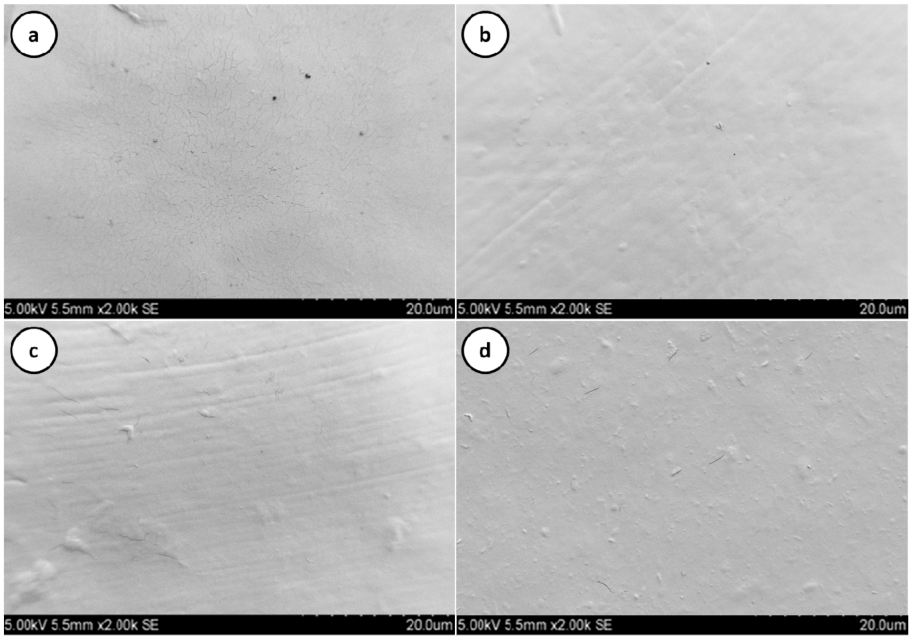


**Figure 2.** SEM micrographs of (**a**) starch-PVA film, (**b**) starch-PVA loaded with 1% CNPs, (**c**) starch-PVA film loaded with 3% CNPs, and (**d**) starch-PVA film loaded with 5% CNPs.

The control film surface was characterised by a smooth and homogeneous structure with some holes, whereas the CNPs addition (1–5% $w/v$) led to a rougher structure, even if more homogeneous and compact, without residual holes. This experimental evidence can

be justified by the interaction between film-forming ingredients and CNPs. Furthermore, CNPs were adequately distributed in all concentrations, suggesting a good interaction between CNPs and the polymer matrix. These results are in agreement with those related to starch films incorporated by CNPs [20], as well as with those reported by Hosseini et al. [29] and Antoniou et al. [27].

Hosseini et al. [29] stated that the obtainment of a homogeneous CNP dispersion within a polymer matrix strongly depends on the nanofiller concentration: low CNP (2% $w/v$) amounts allowed a good dispersion to be obtained without any clumps within the gelatin film matrix, while increasing the level of CNPs (6 to 8% $w/v$) caused a clump and aggregation in film matrix. Antoniou et al. [27] reported that the even distribution of CNPs in Tara gum films improved the homogeneity in the structure of nanocomposite films, leading to better mechanical, physical, and thermal properties of the final films.

### *3.3. Crystallinity of Starch-PVA Films Loaded with CNPs*

XRD patterns of neat and CNP-loaded starch-PVA films are compared in Figure 3.

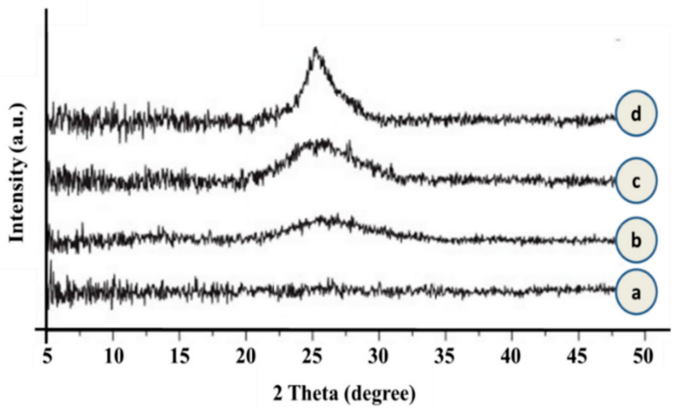


**Figure 3.** XRD patterns of (**a**) starch-PVA film, (**b**) starch-PVA loaded with 1% CNPs, (**c**) starch-PVA film loaded with 3% CNPs, and (**d**) starch-PVA film loaded with 5% CNPs.

As expected, the XRD spectrum of neat starch-PVA film was completely flat due to its amorphous structure. In the case of composite films, a peak at 2Theta 24° was revealed. This peak transitioned from broad to slightly sharp and showed a higher intensity with the addition of CNPs from 1 to 5 % $w/v$. Therefore, it could be due to the presence of CNPs as crystallization inducers within the nanocomposite matrix. These results show that the addition of CNPs in lower amounts had no significant influence on the crystallinity of nanocomposites, but an increase in the addition of nanoparticles improved the crystallinity and the physical properties of the films. By increasing the addition of CNPs in the matrix of starch-PVA films (5% $w/v$), the intensity of peaks increased, while their positions remained unacted. The emerged peak due to the addition of CNPs could be attributed to the decreased crystallinity of nanocomposite films and cause a more regular structure and arrangement [31].

### *3.4. Thermal Properties of Nanocomposite Films*

The weaker thermal stability of biopolymers, particularly natural ones, compared to petroleum-based polymers is one of the main reasons for their limited application in the packaging sector [1,8]. Therefore, to improve their thermal behavior, it is possible to blend them with different polymers and/or to add suitable fillers. The acquired thermal properties of neat and starch-PVA films are compared in Table 1.

**Table 1.** Thermal properties of starch-PVA-based films.

| Sample | Glass Transition Temperature (°C) | Melting Enthalpy (J $g^{-1}$) | Melting Temperature (°C) |
|---|---|---|---|
| Starch-PVA 40:60 (SP) | 146.0 ± 2.2 [a] | 31.3 ± 0.7 [c] | 180.2 ± 1.9 [a] |
| SP+1% CNPs | 141.2 ± 1.5 [b] | 32.1 ± 0.9 [c] | 184.9 ± 2.6 [a] |
| SP+3% CNPs | 135.1 ± 2.7 [c] | 36.6 ± 1.6 [b] | 176.6 ± 1.5 [b] |
| SP+5% CNPs | 130.5 ± 3.0 [c] | 41.5 ± 1.1 [a] | 173.9 ± 1.2 [b] |

Starch-PVA 40:60 (or SP as control film sample), starch-PVA loaded with 1% CNPs (SP+1% CNPs), starch-PVA film loaded with 3% CNPs (SP+3% CNPs), and starch-PVA film loaded with 5% CNPs (SP+5% CNPs). Results are presented as the mean ± standard deviation. Different letters in each column indicate statistically significant differences at $p < 0.05$.

A progressive decrease of the glass transition temperature was revealed when increasing the CNP loading amount, in agreement with previous works related to polyethylene (PE)- and polylactide acid (PLA)-based nanocomposites [8,32] and to CNP-loaded gelatin or starch [29,33]. This experimental evidence has been ascribed to the microstructure of the films and, in particular, to the nanofillers' positioning in free intramolecular voids of the polymer matrix [8], as well as to the higher mobility of their polymer chains [34]. The melting point ($T_m$) and melting enthalpy ($\Delta H_m$) also strongly influence the thermal behaviour. As seen in Table 1, the films' melting temperature is reduced by the addition of the CNPs, in particular, from 180.2 to 173.9 °C in the case of neat and 5% loaded starch-PVA films. Concerning the melting enthalpy, a gradual increase was recorded with the increment of the CNP amount. This finding was associated with a higher crystallinity degree and is in agreement with XRD results (Figure 3), suggesting a good filler dispersion [31], as supported by the related SEM micrographs (Figure 2).

### *3.5. Mechanical Properties*

The measured mechanical properties are reported in Figure 4. As depicted, the addition of CNPs strongly influences both the tensile strength (MPa) and the elongation at break (%) of starch-PVA films. In detail, the tensile strength increased from 35 MPa for the control film sample to 47 MPa for films loaded with 5% CNPs, suggesting good interphase between CNPs and the starch-PVA matrix due to the compatibility between the chitosan and starch-PVA polymeric structures. This is likely owing to the nanofillers' entanglement and the development of the hydrogen bonding arrangement [24,35,36]. The ultimate tensile strength enhancement is associated with the crystallinity degree increase with the CNP amount, as evidenced by the XRD (Figure 3) and DSC (Table 1) data.

As expected, the EAB of nanocomposite films decreased with the CNP loading amount: for example, starch-PVA films containing 5% CNPs presented 40% lower EAB than the control films. The decrease in EAB of the films is a result of the reduction in flexibility of the films. The decrease in free voids between polymer chains is due to an increase in intermolecular chains and a reduction in the consistency of the polymer matrix due to the presence of NPs [22,31]. The same trend was highlighted by Babaee et al. [26] in the case of a plasticized starch (PS)-based film loaded with different amounts of CNPs (1, 2, 3, and 4%). Similarly, De Moura et al. [28] evaluated the influence of the CNPs' diameter size on the mechanical properties of modified cellulose films. In agreement, they reported that the addition of CNPs with an average diameter of 110–221 nm resulted in an increase in the films' TS and a decrease in the EAB, whereas, on the other hand, the addition of CNPs with a particle size of 85 nm increased both the TS and EAB of the films.

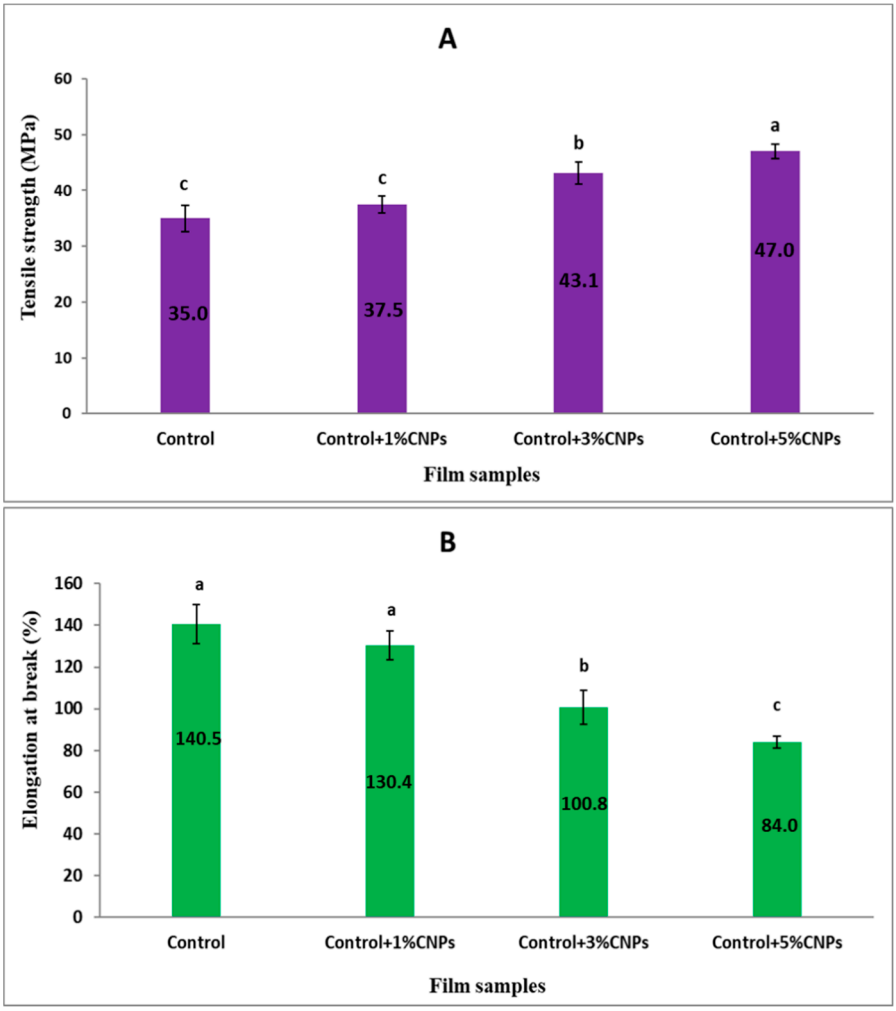


**Figure 4.** (**A**) Tensile strength and (**B**) elongation at break of neat and CNP-loaded starch-PVA films. Starch-PVA 40:60 (control film sample), starch-PVA loaded with 1% CNPs (control + 1% CNPs), starch-PVA film loaded with 3% CNPs (control + 3% CNPs), and starch-PVA film loaded with 5% CNPs (control + 5% CNPs). Different letters in each diagram indicate statistically significant differences at $p < 0.05$.

As expected, the EAB of nanocomposite films decreased with the CNP loading amount: for example, starch-PVA films containing 5% CNPs presented 40% lower EAB than the control films. The decrease in EAB of the films is a result of the reduction in flexibility of the films. The decrease in free voids between polymer chains is due to an increase in intermolecular chains and a reduction in the consistency of the polymer matrix due to the presence of NPs [22,31]. The same trend was highlighted by Babaee et al. [26] in the case of a plasticized starch (PS)-based film loaded with different amounts of CNPs (1, 2, 3, and 4%). Similarly, De Moura et al. [28] evaluated the influence of the CNPs' diameter size on the mechanical properties of modified cellulose films. In agreement, they reported that the addition of CNPs with an average diameter of 110–221 nm resulted in an increase in the films' TS and a decrease in the EAB, whereas, on the other hand, the addition of CNPs with a particle size of 85 nm increased both the TS and EAB of the films.

### *3.6. Physical Properties of Nanocomposite Films*

The film thickness is affected by the film-forming production and the drying method. No significant differences between the films thicknesses were detected, which ranged between 66 to 70 μm (Table 2).

**Table 2.** Physical properties of starch-PVA nanocomposite films loaded with different amounts of CNPs.

| Sample | Thickness (mm) | Water Solubility | WVP (g·mm/kPa·h·m$^2$) | Total Color Differences (ΔE) | Opacity |
|---|---|---|---|---|---|
| Starch-PVA 40:60 (SP) | 0.066 ± 0.002 $^a$ | 79.0 ± 3.2 $^a$ | 0.41 ± 0.02 $^a$ | 3.55 ± 0.11 $^c$ | 0.47 ± 0.04 $^a$ |
| SP+1% CNPs | 0.067 ± 0.003 $^a$ | 77.6 ± 1.2 $^a$ | 0.38 ± 0.03 $^a$ | 3.75 ± 0.18 $^c$ | 0.79 ± 0.08 $^b$ |
| SP+3% CNPs | 0.069 ± 0.002 $^a$ | 74.1 ± 1.3 $^b$ | 0.33 ± 0.01 $^b$ | 4.08 ± 0.08 $^b$ | 1.34 ± 0.19 $^c$ |
| SP+5% CNPs | 0.070 ± 0.003 $^a$ | 71.8 ± 0.5 $^c$ | 0.28 ± 0.03 $^c$ | 4.37 ± 0.12 $^a$ | 1.77 ± 0.29 $^d$ |

Starch-PVA 40:60 (or SP as control film sample), starch-PVA loaded with 1% CNPs (SP+1% CNPs), starch-PVA film loaded with 3% CNPs (SP+3% CNPs), and starch-PVA film loaded with 5% CNPs (SP+5% CNPs). Results are presented as the mean ± standard deviation. Different letters in each column indicate statistically significant differences at $p < 0.05$.

The solubility of the films is one of the main characteristics of edible/biodegradable films, as some of the food products have a high water activity, and the packaging film will be in contact with them [36]. The water solubility (WS) of films represents the polymer's affinity for water molecules [37]. As shown in Table 2, the WS of neat starch-PVA films in distilled water was 79% and was significantly reduced by the addition of CNPs into the films at 3 and 5% $w/v$. The decrease in WS of nanocomposite films can be attributed to the formation of hydrogen bonds between polymers and CNPs, which cannot be disrupted by the water molecules [29]. De Moura et al. [28] reported a similar observation, highlighting a remarkable WS decrease of methylcellulose films as a consequence of increasing CNPs.

The WVP values of the starch-PVA nanocomposite films significantly decreased by adding CNPs into the film matrix (Table 2). Indeed, the WVP of neat starch-PVA films was 0.41 g·mm/kPa·h·m$^2$ and dropped to 0.28 g·mm/kPa·h·m$^2$ due to the addition of CNPs up to 5% $w/v$. This experimental result can be ascribed to the CNPs' ability to increase the polymer structure compactness by placing themselves between voids in the polymer matrix, as evidenced by SEM micrographs (Figure 2), and, thus, to reduce the permeation of water molecules from the polymer matrix [33]. Indeed, it is well known that the WVP of the films is generally affected by the polymer nature, the manufacturing process, the ingredients/additives used for the film formation, the presence of voids, cracks and the polymer matrix homogeneity [38].

The color characterization of films to be potentially used for the packaging of food materials is pivotal since it significantly impacts consumer acceptance of the packaging. The color change in natural polymers is generally influenced by the biopolymer nature, the film-forming process, the pH of the film-forming solution, the presence of plasticizers, nanoparticles, and thermal processing. The results presented in Table 2 show that by the addition of CNPs, the color parameters of the films significantly increased ($p \leq 0.05$), decreasing their lightness (L* value). Films containing 3 and 5% CNPs presented the lowest L* value. Similarly, Antoniou et al. [27] reported that the yellow index of the tara gum films containing CNPs increased mainly due to the yellow color of the CNPs extracted from crap's skin.

Another important parameter for the selection of edible and biodegradable films for different applications is the opacity, since it can also affect the acceptance of products by consumers [39]. From the data in Table 2, it is evident that the opacity significantly increased with the amount of CNPs in the films. This experimental evidence can be ascribed to NPs agglomeration, which reduced the light transmittance from the polymer structure. Similar observations were also reported for CNPs-loaded fish gelatin films [29] and CNPs-loaded cellulose films [40].

### *3.7. Antimicrobial Properties of the Films*

In Figure 5, the pictures of the inhibition zones revealed in the case of agar disc diffusion tests against the selected pathogen microorganisms, i.e., *E. coli*, *S. typhimurium*, and *S. aureus*, are compared, and the evaluation of the antibacterial action is reported

in Table 3 on the basis of the inhibitory area size. As expected, no inhibition zone was evidenced in the case of the neat starch/PVA film, whereas the composite samples were characterized by a progressive increment of the inhibition zone diameter with the CNP concentration.

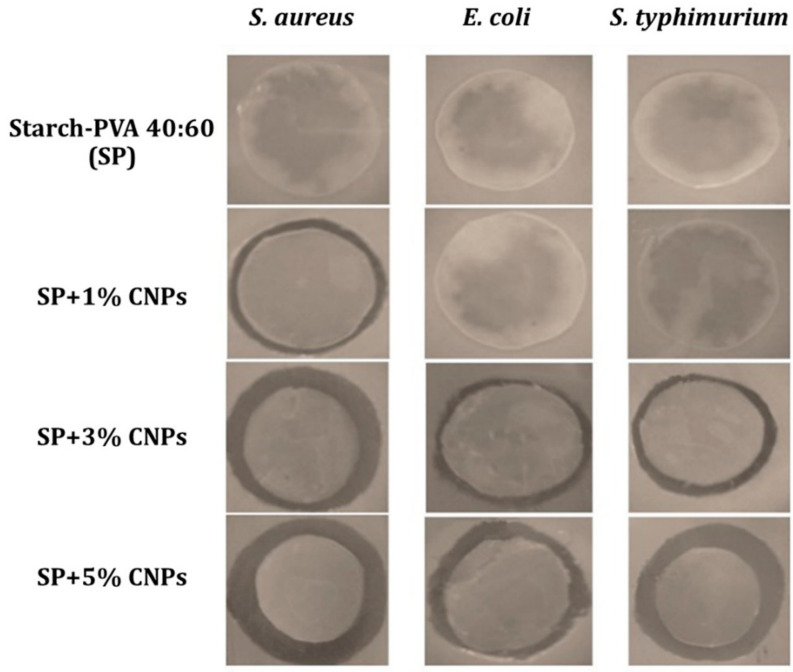


**Figure 5.** Pictures of the inhibition zones revealed in the case of agar diffusion test against *S. aureus*, *E. coli* and *S. typhimurium*. Starch-PVA 40:60 (or SP as control film sample), starch-PVA loaded with 1% CNPs (SP+1% CNPs), starch-PVA film loaded with 3% CNPs (SP+3% CNPs), and starch-PVA film loaded with 5% CNPs (SP+5% CNPs).

**Table 3.** Antibacterial properties of starch-PVA-based films.

| | Inhibition Zone against Selected Bacteria (mm) | | |
|---|---|---|---|
| **Sample** | ***S. aureus*** | ***E. coli*** | ***S. typhimurium*** |
| Starch-PVA 40:60 (SP) | - | - | - |
| SP+1% CNPs | $6.37 \pm 0.79^{c}$ | - | - |
| SP+3% CNPs | $9.35 \pm 0.92^{b}$ | $7.45 \pm 0.63^{b}$ | $7.02 \pm 0.36^{b}$ |
| SP+5% CNPs | $11.78 \pm 1.06^{a}$ | $9.40 \pm 0.81^{a}$ | $8.90 \pm 0.74^{a}$ |

- No inhibitory effect. Starch-PVA 40:60 (or SP as control film sample), starch-PVA loaded with 1% CNPs (SP+1% CNPs), starch-PVA film loaded with 3% CNPs (SP+3% CNPs), and starch-PVA film loaded with 5% CNPs (SP+5% CNPs). Results are presented as the mean ± standard deviation. Different letters in each column indicate statistically significant differences at $p < 0.05$.

In detail, the 1% CNPs addition was only efficient at reducing the growth of *S. aureus*. By increasing the CNPs concentration up to 3–5%, a progressive antibacterial activity was revealed. These experimental findings confirmed that the antimicrobial features were provided by the addition of CNPs, in agreement with previous studies [31]. CNPs can act as antimicrobial agents due to their hydrophobic and chelating nature in pH higher than pKa or neutral pH [41]. A partial and medium inhibitory effect was observed against *E. coli* and *S. typhimurium* for 3 and 5% CNPs, respectively, and a high inhibitory (11.78 mm) action against the *S. aureus* growth was seen in both cases. These experimental findings confirm the higher inhibitory activity of CNPs against Gram-positive bacteria compared to Gram-negative bacteria. Hosseinnejad and Jafari [42] reported that Gram-positive bacteria

have a greater capability to form electrostatic bonds between their cellular wall and CNPs functional groups, mainly due to the thick peptidoglycan layer of Gram-positive bacteria formed from teichoic acids. Phosphate groups with a negative charge can form electrostatic bonds with cationic particles such as chitosan or their derivatives. CNPs can modify the cellular membrane due to their negative charge, are able to inactivate the cell membrane permeability by connecting to the microorganism DNA, and can cause the cellular death by disrupting the cell reproduction [43,44]. These higher antimicrobial properties of CNPs against Gram-positive microorganisms were also reported by Hosseini et al. [29] and Osheba et al. [45] (against *S. aureus* and coliform bacteria for 2–4% *w*/*v* CNPs amounts), as well as by Shojaei et al. [46] (against *L. monocytogenes*, *S. aureus* in the case of whey protein isolate-HPMC films containing 5% CNPs).

## 4. Conclusions

In the current study, composite polyvinyl alcohol (PVA):starch (60:40) films containing spherical-shaped CNPs (average diameter of 100 nm) are proposed as a promising alternative to the petroleum-based films traditionally used for food packaging applications in order to reduce their environmental impact. The influence of additional CNPs on the microstructural, chemico-physical, thermal, mechanical and antimicrobial properties of PVA-starch-based films was investigated. SEM observation revealed a compact surface for the nanocomposite films without the presence of cracks or holes. The addition of CNPs reduced both the glass transition (from 146 °C for neat starch-PVA to 130 °C for SP+5% CNPs) and the melting temperatures (from 180 °C for neat starch-PVA to 174 °C for SP+5% CNPs) and of the starch-PVA films. Mechanical analysis of the films evidenced a remarkable increment of the tensile strength from 35 MPa (control sample) to 47 MPa (5% CNPs loaded sample), associated with a reduction in the elongation at the break up to 40% due to the addition of the highest CNPs amount. On the other hand, no significant differences between control and nanocomposite films containing 1% CNPs were observed. As expected, the addition of CNPs into the films significantly reduced their WVP (from 0.41 g·mm/kPa·h·m$^2$ for neat starch-PVA films to 0.28 g·mm/kPa·h·m$^2$ for SP+5% CNPs), as well as the water solubility (from 79% for neat starch-PVA films to 71.8% for SP+5% CNPs), while the opacity (from 0.47 for neat starch-PVA films to 1.77 for SP+5% CNPs) increased. The color analysis of the films depicted that the lightness (L*) of films significantly reduced by increasing the CNPs concentration. This reduction in lightness was more significant for the higher CNP concentrations, i.e., 3 and 5% *w*/*v*. The antimicrobial analysis of nanocomposite films against Gram-positive (*S. aureus*) and Gram-negative bacteria (*E. coli* and *S. typhimurium*) confirmed a higher inhibitory effect of CNPs against Gram-positive than Gram-negative bacteria. All the collected results demonstrated the high potential of using CNPs as a reinforcement agent, improving the starch-PVA films in terms of physical and mechanical properties and making them promising candidates for the food packaging industry.

**Author Contributions:** Conceptualization, F.G. and A.T.-G.; methodology, Y.G.; software, Y.G.; validation, F.G., A.T.-G. and I.C.; formal analysis, D.K.; investigation, Y.G.; resources, F.S.; data curation, F.S.; writing—original draft preparation, Y.G. and D.K.; writing—review and editing, F.G. and I.C.; visualization, Y.G.; supervision, A.T.-G. and F.S.; project administration, F.G.; funding acquisition, A.T.-G. and I.C. All authors have read and agreed to the published version of the manuscript.

**Funding:** This research received no external funding.

**Conflicts of Interest:** The authors declare no conflict of interest.

## References

1. Garavand, F.; Rouhi, M.; Razavi, S.H.; Cacciotti, I.; Mohammadi, R. Improving the integrity of natural biopolymer films used in food packaging by crosslinking approach: A review. *Int. J. Biol. Macromol.* **2017**, *104*, 687–707. [CrossRef]
2. Khodaei, D.; Álvarez, C.; Mullen, A.M. biodegradable packaging materials from animal processing co-products and wastes: An overview. *Polymers* **2021**, *13*, 2561. [CrossRef]

3. Van Der Zee, M. 1. Methods for evaluating the biodegradability of environmentally degradable polymers. In *Handbook of Biodegradable Polymers*; De Gruyter: Berlin, Germany, 2020; pp. 1–22.
4. Hadidi, M.; Jafarzadeh, S.; Forough, M.; Garavand, F.; Alizadeh, S.; Salehabadi, A.; Mousavi Khaneghah, A.; Jafari, S.M. Plant protein-based food packaging films; recent advances in fabrication, characterization, and applications. *Trends Food Sci. Technol.* **2022**, *120*, 154–173. [CrossRef]
5. Khodaei, D.; Hamidi-Esfahani, Z.; Lacroix, M. Gelatin and low methoxyl pectin films containing probiotics: Film characterization and cell viability. *Food Biosci.* **2020**, *36*, 100660. [CrossRef]
6. Bahrami, R.; Zibaei, R.; Hashami, Z.; Hasanvand, S.; Garavand, F.; Rouhi, M.; Jafari, S.M.; Mohammadi, R. Modification and improvement of biodegradable packaging films by cold plasma; a critical review. *Crit. Rev. Food Sci. Nutr.* **2020**, 1–15. [CrossRef]
7. Cacciotti, I.; Lombardelli, C.; Benucci, I.; Esti, M. Clay/chitosan biocomposite systems as novel green carriers for covalent immobilization of food enzymes. *J. Mater. Res. Technol.* **2019**, *8*, 3644–3652. [CrossRef]
8. Garavand, F.; Cacciotti, I.; Vahedikia, N.; Rehman, A.; Tarhan, Ö.; Akbari-Alavijeh, S.; Shaddel, R.; Rashidinejad, A.; Nejatian, M.; Jafarzadeh, S. A comprehensive review on the nanocomposites loaded with chitosan nanoparticles for food packaging. *Crit. Rev. Food Sci. Nutr.* **2020**, 1–34. [CrossRef]
9. Mohammadi Nafchi, A.; Moradpour, M.; Saeidi, M.; Alias, A.K. Thermoplastic starches: Properties, challenges, and prospects. *Starch-Stärke* **2013**, *65*, 61–72. [CrossRef]
10. Khan, B.; Bilal Khan Niazi, M.; Samin, G.; Jahan, Z. Thermoplastic starch: A possible biodegradable food packaging material—A review. *J. Food Process Eng.* **2017**, *40*, e12447. [CrossRef]
11. Verbeek, C.; Bier, J. Synthesis and characterization of thermoplastic agro-polymers. In *Handbook of Applied Biopolymer Technology*; RSC Publishing: Cambridge, UK, 2011; pp. 197–242.
12. Mirzaei-Mohkam, A.; Garavand, F.; Dehnad, D.; Keramat, J.; Nasirpour, A. Optimisation, antioxidant attributes, stability and release behaviour of carboxymethyl cellulose films incorporated with nanoencapsulated vitamin E. *Prog. Org. Coat.* **2019**, *134*, 333–341. [CrossRef]
13. Mirzaei-Mohkam, A.; Garavand, F.; Dehnad, D.; Keramat, J.; Nasirpour, A. Physical, mechanical, thermal and structural characteristics of nanoencapsulated vitamin E loaded carboxymethyl cellulose films. *Prog. Org. Coat.* **2020**, *138*, 105383. [CrossRef]
14. Musetti, A.; Paderni, K.; Fabbri, P.; Pulvirenti, A.; Al-Moghazy, M.; Fava, P. Poly (vinyl alcohol)-based film potentially suitable for antimicrobial packaging applications. *J. Food Sci.* **2014**, *79*, E577–E582. [CrossRef]
15. Piergiovanni, L.; Limbo, S. *Food Packaging Materials*; Springer: Zürich, Switzerland, 2016; pp. 46–50.
16. Azizi-Lalabadi, M.; Garavand, F.; Jafari, S.M. Incorporation of silver nanoparticles into active antimicrobial nanocomposites: Release behavior, analyzing techniques, applications and safety issues. *Adv. Colloid Interface Sci.* **2021**, *293*, 102440. [CrossRef]
17. Benucci, I.; Lombardelli, C.; Cacciotti, I.; Liburdi, K.; Nanni, F.; Esti, M. Chitosan beads from microbial and animal sources as enzyme supports for wine application. *Food Hydrocoll.* **2016**, *61*, 191–200. [CrossRef]
18. Jamróz, E.; Kulawik, P.; Kopel, P. The effect of nanofillers on the functional properties of biopolymer-based films: A review. *Polymers* **2019**, *11*, 675. [CrossRef]
19. De Azeredo, H.M. Nanocomposites for food packaging applications. *Food Res. Int.* **2009**, *42*, 1240–1253. [CrossRef]
20. Chang, P.R.; Jian, R.; Yu, J.; Ma, X. Fabrication and characterisation of chitosan nanoparticles/plasticised-starch composites. *Food Chem.* **2010**, *120*, 736–740. [CrossRef]
21. Chang, P.R.; Jian, R.; Yu, J.; Ma, X. Starch-based composites reinforced with novel chitin nanoparticles. *Carbohydr. Polym.* **2010**, *80*, 420–425. [CrossRef]
22. Khazaei, A.; Nateghi, L.; Zand, N.; Oromiehie, A.; Garavand, F. Evaluation of physical, mechanical and antibacterial properties of pinto bean starch-polyvinyl alcohol biodegradable films reinforced with cinnamon essential oil. *Polymers* **2021**, *13*, 2778. [CrossRef]
23. Hosseini, S.F.; Zandi, M.; Rezaei, M.; Farahmandghavi, F. Two-step method for encapsulation of oregano essential oil in chitosan nanoparticles: Preparation, characterization and in vitro release study. *Carbohydr. Polym.* **2013**, *95*, 50–56. [CrossRef] [PubMed]
24. Dehnad, D.; Mirzaei, H.; Emam-Djomeh, Z.; Jafari, S.-M.; Dadashi, S. Thermal and antimicrobial properties of chitosan–nanocellulose films for extending shelf life of ground meat. *Carbohydr. Polym.* **2014**, *109*, 148–154. [CrossRef] [PubMed]
25. Khodaei, D.; Oltrogge, K.; Hamidi-Esfahani, Z. Preparation and characterization of blended edible films manufactured using gelatin, tragacanth gum and, Persian gum. *LWT-Food Sci. Technol.* **2020**, *117*, 108617. [CrossRef]
26. Babaee, M.; Garavand, F.; Rehman, A.; Jafarazadeh, S.; Amini, E.; Cacciotti, I. Biodegradability, physical, mechanical and antimicrobial attributes of starch nanocomposites containing chitosan nanoparticles. *Int. J. Biol. Macromol.* **2022**, *195*, 49–58. [CrossRef] [PubMed]
27. Antoniou, J.; Liu, F.; Majeed, H.; Zhong, F. Characterization of tara gum edible films incorporated with bulk chitosan and chitosan nanoparticles: A comparative study. *Food Hydrocoll.* **2015**, *44*, 309–319. [CrossRef]
28. De Moura, M.; Avena-Bustillos, R.; McHugh, T.; Krochta, J.; Mattoso, L. Properties of novel hydroxypropyl methylcellulose films containing chitosan nanoparticles. *J. Food Sci.* **2008**, *73*, N31–N37. [CrossRef]
29. Hosseini, S.F.; Rezaei, M.; Zandi, M.; Farahmandghavi, F. Fabrication of bio-nanocomposite films based on fish gelatin reinforced with chitosan nanoparticles. *Food Hydrocoll.* **2015**, *44*, 172–182. [CrossRef]
30. Cacciotti, I.; Mori, S.; Cherubini, V.; Nanni, F. Eco-sustainable systems based on poly (lactic acid), diatomite and coffee grounds extract for food packaging. *Int. J. Biol. Macromol.* **2018**, *112*, 567–575. [CrossRef] [PubMed]

31. Vahedikia, N.; Garavand, F.; Tajeddin, B.; Cacciotti, I.; Jafari, S.M.; Omidi, T.; Zahedi, Z. Biodegradable zein film composites reinforced with chitosan nanoparticles and cinnamon essential oil: Physical, mechanical, structural and antimicrobial attributes. *Colloid. Surf. B Biointerfaces* **2019**, *177*, 25–32. [CrossRef]
32. Hijazi, N.; Le Moigne, N.; Rodier, E.; Sauceau, M.; Vincent, T.; Benezet, J.C.; Fages, J. Biocomposite films based on poly (lactic acid) and chitosan nanoparticles: Elaboration, microstructural and thermal characterization. *Polym. Eng. Sci.* **2019**, *59*, E350–E360. [CrossRef]
33. Martelli, M.R.; Barros, T.T.; de Moura, M.R.; Mattoso, L.H.; Assis, O.B. Effect of chitosan nanoparticles and pectin content on mechanical properties and water vapor permeability of banana puree films. *J. Food Sci.* **2013**, *78*, 98–104. [CrossRef]
34. Liu, L.; Lin, W.-J.; Liu, H.-Z.; Shi, A.-M.; Hu, H.; Nasir, M.N.; Deleu, M.; Wang, Q. Effect of xylose on the structural and physicochemical properties of peanut isolated protein based films. *RSC Adv.* **2017**, *7*, 52357–52365. [CrossRef]
35. Gómez-Estaca, J.; Balaguer, M.P.; Gavara, R.; Hernandez-Munoz, P. Formation of zein nanoparticles by electrohydrodynamic atomization: Effect of the main processing variables and suitability for encapsulating the food coloring and active ingredient curcumin. *Food Hydrocoll.* **2012**, *28*, 82–91. [CrossRef]
36. Abdollahi, M.; Rezaei, M.; Farzi, G. A novel active bionanocomposite film incorporating rosemary essential oil and nanoclay into chitosan. *J. Food Eng.* **2012**, *111*, 343–350. [CrossRef]
37. Kim, S.J.; Ustunol, Z. Sensory attributes of whey protein isolate and candelilla wax emulsion edible films. *J. Food Sci.* **2001**, *66*, 909–911. [CrossRef]
38. Vásconez, M.B.; Flores, S.K.; Campos, C.A.; Alvarado, J.; Gerschenson, L.N. Antimicrobial activity and physical properties of chitosan–tapioca starch based edible films and coatings. *Food Res. Int.* **2009**, *42*, 762–769. [CrossRef]
39. Bilbao-Sainz, C.; Avena-Bustillos, R.J.; Wood, D.F.; Williams, T.G.; McHugh, T.H. Composite edible films based on hydroxypropyl methylcellulose reinforced with microcrystalline cellulose nanoparticles. *J. Agric. Food Chem.* **2010**, *58*, 3753–3760. [CrossRef] [PubMed]
40. Ju, S.; Zhang, F.; Duan, J.; Jiang, J. Characterization of bacterial cellulose composite films incorporated with bulk chitosan and chitosan nanoparticles: A comparative study. *Carbohydr. Polym.* **2020**, *237*, 116167. [CrossRef]
41. Kong, M.; Chen, X.G.; Xing, K.; Park, H.J. Antimicrobial properties of chitosan and mode of action: A state of the art review. *Int. J. Food Microbiol.* **2010**, *144*, 51–63. [CrossRef] [PubMed]
42. Hosseinnejad, M.; Jafari, S.M. Evaluation of different factors affecting antimicrobial properties of chitosan. *Int. J. Biol. Macromol.* **2016**, *85*, 467–475. [CrossRef]
43. Wardani, G.; Sudjarwo, S.A. In vitro antibacterial activity of chitosan nanoparticles against *Mycobacterium tuberculosis*. *Pharmacogn. J.* **2018**, *10*, 162–166. [CrossRef]
44. Divya, K.; Vijayan, S.; George, T.K.; Jisha, M. Antimicrobial properties of chitosan nanoparticles: Mode of action and factors affecting activity. *Fibers Polym.* **2017**, *18*, 221–230. [CrossRef]
45. Osheba, A.; Sorour, M.; Abdou, E.S. Effect of chitosan and chitosannanoparticles as active coating on microbiological characteristics of fish fingers. *J. Agric. Environ. Sci.* **2013**, *2*, 158–169.
46. Shojaei, M.; Eshaghi, M.; Nateghi, L. Characterization of hydroxypropyl methyl cellulose–whey protein concentrate bionanocomposite films reinforced by chitosan nanoparticles. *J. Food Process. Preserv.* **2019**, *43*, e14158. [CrossRef]